Vision Research 171 (2020) 17–30

Contents lists available at ScienceDirect

Vision Research

journal homepage: www.elsevier.com/locate/visres

Comparative study of the visual system of two psammophilic lizards (*Scincus scincus* & *Eumeces schneideri*)

Jérôme Canei[a], Carmen Burtea[b], Denis Nonclercq[a,*]

[a] Laboratory of Histology, Biosciences Institute, Faculty of Medicine and Pharmacy, University of Mons, 23, Place du Parc, B-7000 Mons, Belgium
[b] Department of General, Organic and Biomedical Chemistry, NMR and Molecular Imaging Laboratory, University of Mons, B-7000 Mons, Belgium

ARTICLE INFO

Keywords:
Skinks
Eye
Retina
Immunohistochemistry
MRI
Scincidae

ABSTRACT

Sand deserts are common biotopes on the earth's surface. Some specialized vertebrate species have colonized these ecological habitats by living buried in the sand. Among these so called psammophilic species are the Scincidae sand dune living species *Scincus scincus* and *Eumeces schneideri*. These two skinks share a relatively similar behavioral ecology by living buried in sand, almost all the time for *S. scincus* and at least for some part of the day for *E. schneideri*. The visual system of these two lizards was investigated by histological, immunohistochemical, Magnetic Resonance Imaging (MRI) and morphometric techniques. Both skink species exhibit a retina lacking fovea, composed predominantly of cones presenting two types of oil droplets (pale blue-green and colorless). Both species possess a subset of rod like-photoreceptors (about 1 rod for 30 cones) evidenced by anti-rhodopsin immunoreactivity. A ratio 1:1–1:2 between ganglion cells and photoreceptors points to a linear connection (photoreceptors/bipolar neurons/ganglion cells) in the retina and indicates that both skinks more likely possess good visual acuity, even in the peripheral retina. The MRI analysis revealed differences between the species concerning the eye structures, with a more spherical eye shape for *S. scincus*, as well as a more flattened lens. The relative lens diameter of both species seems to correspond to a rather photopic pattern. Beside the fact that *S. scincus* and *E. schneideri* have different lifestyles, their visual capacities seem similar, and, generally speaking, these two psammophilic species theoretically exhibit visual capacities not far away from non-fossorial species.

1. Introduction

Light is a major environmental factor which has exerted a powerful selective pressure on living creatures. This factor has led to various evolutionary innovations, including the appearance of highly complex and specialized organs: the eyes. Vertebrates, including lizard species described in this article, possess very efficient paired chambered eyes with two lenses (Fernald, 2004).

Vertebrates have two types of photoreceptors at the retina level: cones and rods. The first are related to visual acuity and color vision, the second to visual sensitivity (Gerhing, 2014). These two types of photoreceptors operate in different light intensity ranges. The cones being active at high intensity while the rods are specialized in perception under low light intensities. However, there is a range of intermediate intensities where these two types of photoreceptor are active. Photopic is the light intensity range in which vision is purely cone-mediated corresponding generally to daylight conditions, scotopic is the range of low light intensities encountered generally in nocturnal conditions in which it is rod-mediated, and mesopic vision is the in-between in which both photoreceptor types are functional. Naturally, this ranges vary between species (Kelber & Lind, 2010; Kelber, Yovanovich, & Olsson, 2017). Concerning the color perception, it requires the presence of at least two different spectral photoreceptor types (Kelber, Vorobyev, & Osorio, 2003; Yovanovich et al., 2017). Depending on the species, vertebrates have monochromatic vision (making them color-blind – like for most aquatic mammals) (Peichl, Behrmann, & Kroger, 2001), dichromatic vision (observed in a large number of terrestrial mammals) (Kelber et al., 2003; Peichl et al., 2001), and trichromatic vision (like for catarrhine primates, geckos and crocodiles) (Kelber et al., 2003). Moreover, many teleost fishes (Neumeyer, 1992), reptiles (Ammermüller, Muller, & Kolb, 1995) and birds (Chen & Goldsmith, 1986; Kelber, 2019) have tetrachromatic vision. Finally, regarding the proportion and the nature of Squamata photoreceptors, the different lizard families of Iguanidae, Chameleonidae, Agamidae, Scincidae, Lacertidae, Anguidae, Pygopodidae and Varanidae commonly possess a pure cone retina, as referred to in the

* Corresponding author at: Laboratory of Histology, University of Mons 6, Avenue du Champ de Mars, Mons, 7000, Belgium.
E-mail address: denis.nonclercq@umons.ac.be (D. Nonclercq).

https://doi.org/10.1016/j.visres.2020.04.004
Received 21 November 2019; Received in revised form 17 April 2020; Accepted 17 April 2020

study of Röll (2001a).

In bright light conditions, numerous vertebrate species have developed high visual acuity involving retinal specific structures as the fovea, a retinal pit located in the optical axis with high cone density. Foveae are present in a great number of vertebrates, including mammals (Rodieck, 1998), birds, reptiles, (Moore et al., 2017) and even Teleost fishes (Collin & Collin, 1999; Easter, 1992). Some reptile species, like the well-studied group of lizards of the genus *Anolis*, possess a complex visual system including two morphologically different and spatially separated foveae (Fite & Lister, 1981). Another visual structure is the oil droplets present in cones. These are widespread among diurnal birds and reptiles (Vorobyev, 2003) and act like individual filters of the photoreceptors allowing more acute vision (Stavenga & Wilts, 2014) and erase the flickering effect on the surface of the water (Muntz, 1972; Zeigler & Bischof, 1993). The pigmentation of these structures also seems important, because when pigmented they reduce the light spectrum range reaching the outer segments of the cones and promote the excitation of the specific opsin of the cone. Some cones possess only transparent oil-droplets that improve how light is caught and increase visual sensitivity (Wilby & Roberts, 2017).

Reptiles, and more precisely Squamata, are generally diurnal species (Hall, 2008). The biggest group of nocturnal lizard species are found in the Gekkonidae, but it is noteworthy that their ancestors are believed to have been diurnal (Röll, 2001a). Beside these general adaptations to light conditions, numerous adaptations have appeared among vertebrates to cope with peculiar lifestyles, like for fossorial species. Among mammals, some fossorial species, like the rodent *Spalax ehrenbergi*, have atrophied eyes and have lost some types of photoreceptors (Hunt & Collin, 2014). These features are also encountered in Squamata, like in fossorial Amphisbaenia, which have some common characteristics linked to this specific lifestyle, such as a reduced eyeball size and a lens with amorphous nucleate cells (Foureaux et al., 2010). It is noteworthy that atrophied eyes are also found in burrowing caecilian amphibians (Mohun et al., 2010).

Our study focuses on two species of Scincidae family: *Scincus scincus* (Linnaeus, 1758) and *Eumeces schneideri* (Daudin, 1802). These two skinks are phylogenetically closely related (Pyron, Burbrink, & Wiens, 2013). Moreover, they share a common geographical distribution, from the Mediterranean coast to Saheli band through all Sahara desert and also in the Arabian peninsula into Sinai, and desertic zones of Syria, Iraq, Jordan and west part of Iran (Arnold & Leviton, 1977; Ayaz, Çiçek, Tok, & Dinçaslan, 2011). The omnivorous sandfish *S. scincus* hunts insects, by the detection of vibratory cues (Hetherington, 1989) in hot deserts composed of few dry shrubs (Attum, Covell, & Eason, 2004). The omnivorous Berber skink (*E. schneideri)* is also found in such biotopes, but with relatively dense vegetation (Allam, Abo-Eleneen, & Othman, 2017). These two diurnal skinks are psammophilic and thus live buried in the sand, almost all the time for *S. scincus* (Stadler et al., 2016) while *E. schneideri* spends more time laps at the surface of the sand during the diurnal period for hunting or mating (Saleh, 1997). The sandfish is famous for its morphological adaptations as a shovel-shaped snout, a subquadrangular cross section of the body, a reduced ear openings and fringed toes and digits allowing to move easily under the sand (sand swimming) (Baumgartner et al., 2008) and for the remarkable properties of its skin which resist the intense abrasion of sand particles (Vihar, Hanisch, & Baumgartner, 2016). To our knowledge, no articles found in the literature have mentioned the visual system of these two burrowing skink species (with the noticeable exception of Khattab, Khattab, Fares, & Zaki, 2004). These authors attest by ultrastructural approach that the retina of the *Eumeces schneideri* is largely dominated by cones with present oil droplet. These cones are only single cone, indeed double cones are not present in this species. On the other hand, Khattab et al. (2004) have observed some scattered rods in the retina of *E. schneideri*. The Scincidae family (Lepidosauria) comprises a vast majority of diurnal species, with a few exceptions. Inside this family, the visual system has been very poorly investigated. Apart from the study of Khattab et al. (2004) cited just above, the few published data on Scincidae's ocular adaptations concern the following species: *Tiliqua rugosa* (Braekevelt, 1989; New, Hemmi, Kerr, & Bull, 2012), *Cryptoblepharus boutonii* (Röll, 2001b), *Acontias orientalis*, *Acontias rieppeli*, *Typhlosaurus vermis* and *Trachylepis punctatissima* (Zhao, Goedhals, Verdú-Ricoy, Jordaan, & Heideman, 2019). Recently, the eye morphology of one burrowing species (*Calyptommatus nicterus*, Gymnophthalmidae) and one surface-dwelling lizard (*Ameivula ocellifera*, Teiidae) has been studied (Yovanovich, Pierotti, Rodrigues, & Grant, 2019). These two species are part of the Infraorder Scincomorpha and belong to two families close to the Scincidae, from a phylogenic point of view (Pyron et al., 2013).

The aim of this study is to compare the eye morphology and retinal structure of burrowing Scincidae to other diurnal members of this family, and to pinpoint the evolutionary adaptations of the eye structure of fossorial psammophilic Scincidae in relation to environmental light conditions. Considering the lifestyle of both studied species, which are restricted to very dim light conditions when they are buried, we could expect that their visual system is more sensitive and scotopic than photopic and acute. However, the Sahara Desert is one of the most illuminated areas on Earth, with a theoretical daylight of approximately 100,000 Lux of illuminance (without clouds) as highlighted by typical calculated values (Kandilli & Ulgen, 2008). We expect that *S. scincus* may have less acute vision compared to the semi-fossorial Berber Skink, which could possess an intermediate visual system adapted to both prey detection (in bright light conditions) and sand diving (with almost no light).

2. Material and methods

2.1. Animals

Three adult individuals (two males and one female) (mean snout–tail length, STL: 16.25 cm ± 2 mm) of the species *Scincus scincus* (Fig. 1a, b) were used in the experiments. These specimens were obtained from the Animal House "Animalerie 2000" (Mouscron, Belgium). Three other adult individuals (three males) (mean snout-tail, STL: 32.66 cm ± 2 mm) of the species *Eumeces schneideri* (Fig. 1c, d) were also used. These specimens were obtained from the Animal House "Reptiles Univers" (Dour, Belgium). The individuals of these two species were maintained in the animal housing facility of the University of Mons (UMONS, Belgium). The animals were treated according to the guidelines specified by the Belgian Ministry of Trade and Agriculture and under the control of the UMONS ethical commission (agreement LA1500021). The lizards were placed individually in terraria (120 × 60 × 60 cm) whose bottoms were covered with a 10–12 cm thick layer of fine sand (with a particle diameter comprised between 0.75 and 1.3 mm). Each terrarium was equipped with an UV rich lamp (5.0 UVB, 26 W; ZooMed®) and an infrared bulb for heating (Ceramic infrared, 60 W; ZooMed®). Both light bulbs were placed at a height of 35 cm. The animals were maintained in a controlled environment with 12 h of daylight and a temperature of 35 °C during the day, and 22 °C at night. The animals were fed with live adult house crickets (*Acheta domesticus*), and vegetables twice a week and received water *ad libitum*. The animals were euthanized by a lethal intramuscular injection of ketamine hydrochloride (200 mg/kg body mass, Ketalar®). Each subject was considered euthanized when it lost the ability to respond to feet and tail pinching. This was done under the control of the UMONS Committee for Survey of Experimental Studies and Animal Welfare.

2.2. Histology

After euthanasia, all individuals were transversally cut at the level of the head-trunk junction. Once the head was isolated, a careful chirurgical removal of the ocular globes was performed. These were then fixed by immersion in Duboscq–Brazil fluid (composition:

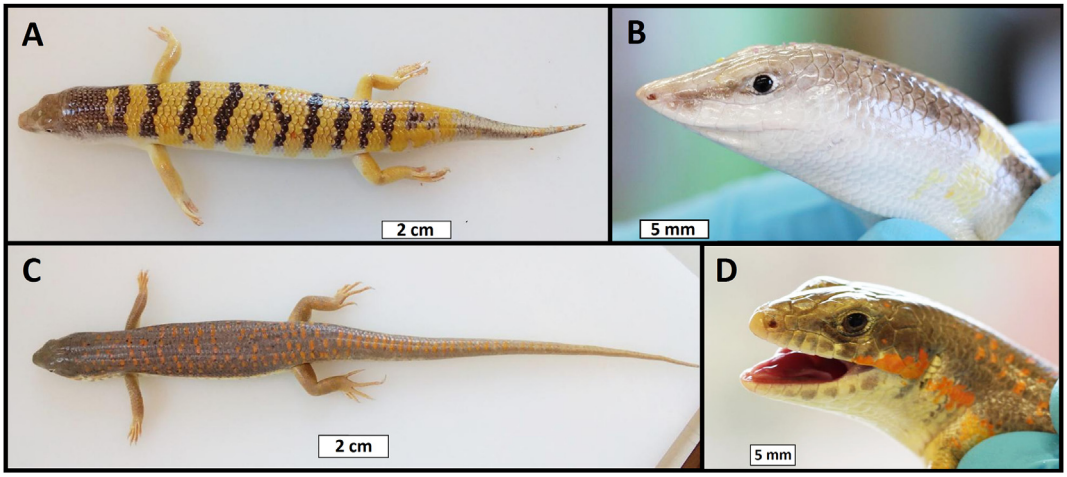

Fig. 1. Anatomical dorsal and lateral views, respectively, of *Scincus scincus* [Sandfish] (A & B) and *Eumeces schneideri* [Berber skink] (C & D).

formalin/acetic acid/ethanol containing 1% picric acid/distilled water, respective proportions: 260/70/425/245 by vol.) for 48 h. The samples, after dehydration and paraffin-embedding, were cut in sagittal serial sections of 5 μm thickness on a Leica® RM 2145 microtome and placed on silane-coated glass slides. After rehydration, the sections were stained with hematoxylin, Orange G and Fast green (Masson's Trichrome stain) to allow histological examination. The tissue sections were observed on a research optical microscope (Leitz® Orthoplan) equipped with a high sensitivity camera (Leica® DFT7000 T, Germany) and pictures were recorded using specialized software (Leica® Application Suite X, LASX, Germany).

2.3. Identification of rods by immunohistochemistry

Serial sections of the eyes of *Scincus scincus* and *Eumeces schneideri* individuals were used to study the photoreceptor typing. Along the optical axis of both species' eyes, three medio-sagittal consecutive sections (passing through the *conus papillaris*) of 5 μm thick were taken and treated for immunostaining of rhodopsin. This allowed us to evaluate the concentration of rod photoreceptors in the different retinal areas and to perform intra- and inter-specific comparisons. Prior to immunostaining, dewaxed sections were rehydrated and rinsed in distilled water. The unmasking of antigenic sites was performed by microwave heating in 0.01 M citrate buffer (pH = 6.2). Sections were warmed up over two consecutive runs (+/−5 min) of microwave heating at a power of 900 W spaced by a 15 min break. The heating was stopped when the first boiling bubbles appeared. After rinsing with distilled water, endogenous peroxidase activity was quenched by a 5 min. exposure to 0.5% H_2O_2. Before applying the primary antibodies, the pretreated sections were rinsed in PBS (0.04 M $Na_2HPO_4.12H_2O$, 0.01 M KH_2PO_4 and 0.12 M NaCl, pH 7.4) and incubated in 0.5% casein (diluted in PBS) for 15 min. in order to quench the background. Tissue sections were incubated with a monoclonal antibody raised against rhodopsin (Rho4D2). This commercial monoclonal antibody was raised in mice and purchased from Abcam® (Cambridge, UK). This primary antibody was used at optimal working dilution (1:50) and histological sections were incubated for one hour at room temperature. After rinsing in PBS, slices were treated with the complex ImmPRESS™ HRP/Anti-MouseIgG/Polymer (Vector®, Burlingame, CA) for 30 min. at room temperature. Bound peroxidase activity was visualized by precipitation of 3.3′ diaminobenzidine (DAB) 0.02% in PBS containing 0.01% H_2O_2. Preparations were counterstained with hemalun and luxol fast blue, dehydrated and mounted with a permanent medium. Controls for the specificity of immunolabeling included the omission of the primary antibody or the substitution of non-immune sera for the primary antibodies. In each case, these controls were negative.

2.4. Evaluation of retinal cell density and ratio (photoreceptors/integrative neurons/ganglion cells) and evaluation of photoreceptor inner segment mean diameter.

For each species (n = 3), retinal cells were counted individually on three consecutive slides (for both species) cut following the medio-sagittal axis (passing through the *conus papillaris*), representing a total scanned area of 6,843,456 μm^2 for *Scincus scincus* and 5,132,592 μm^2 for *Eumeces schneideri*. Three retinal layers were considered: photoreceptors cells, cells of the inner nuclear layer (including bipolar, amacrine and horizontal cells) and ganglion cells. Slides stained by Masson's Trichrome were used and the counting was performed by targeting the nucleus highlighted by the haematoxylin. All the counting measures were done using the free software ImageJ (Image Processing and Analysis in Java, Java 1.6.0). Each slide was divided into four fields, starting from the central retina to the most peripheral zone (at the *ora serrata* junction). The number of each retinal cell type was compared intra- and inter-specifically. Each retinal cell type identified by the localization of its nucleus (photoreceptor nuclei (located in retinal outer nuclear layer) – integrative cell nuclei (located in retinal inner nuclear layer)– ganglion cell nuclei (located in retinal ganglion cell layer)) was counted in two different retinal areas. These counting areas corresponded to the central retina (two central fields) and the peripheral retina (two outmost fields) to investigate intra- and inter-specific differences. The ratio between ganglion cells and photoreceptors was estimated by dividing the former by the latter. We have also estimated the mean diameter (in μm) of the photoreceptors (cones and rods combined), by estimating the width of all photoreceptors at the inner segment level. The diameter assessing was performed by using the same slides that for the pre-mentioned counting. The software ImageJ allowed these measurements.

2.5. Distribution and density of rods and cones

For each species (n = 3), photoreceptor cells were counted individually on three consecutive medio-sagittal eye sections immunolabeled by anti-rhodopsin antibodies following the pre-mentioned immunohistochemistry protocol. The labeled cells being rods and the untargeted cells being cones, we were able to discriminate and estimate the proportion of each photoreceptor type. Intra- and inter-specific comparisons were made between central retina (four fields of 22,750 μm^2 picked in this area) and peripheral retina (four similar fields). In both retinal zones, the specific ratio between rods and cones for each species was compared. Immunolabeled sections were observed on a research optical microscope (Leitz® Orthoplan) equipped with a high sensitivity camera (Leica® DFT7000 T, Germany) and pictures

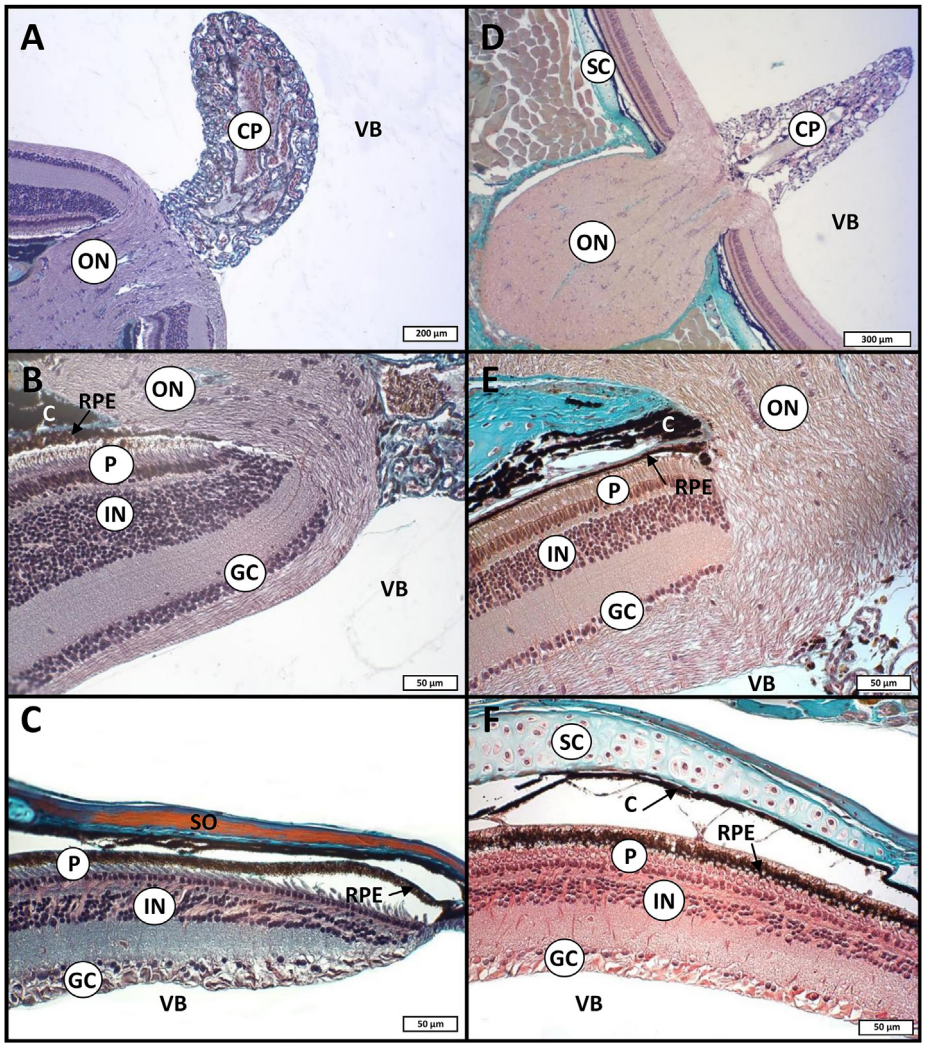

Fig. 2. Histological photographs of main retinal areas of *S. scincus* (A, B, C) and *E. schneideri* (D, E, F). All sections were stained by Masson's Trichrome. Pictures of the *Conus papillaris* and optic nerve (A, D). Low magnification images of the central (B, E) and peripheral retina (C, F). ON: optical nerve, CP: conus papillaris, VB: vitreous body, P: photoreceptors layer, IN: inner nuclear layer (including bipolar, amacrine and horizontal cells), GC: ganglion cells layer, SC: scleral cartilage, SO: Scleral ossicles, C: Choroid, RPE: Retinal pigment epithelium.

were recorded using specialized software (Leica® Application Suite X, LAS X, Germany).

2.6. Cornea morphometric analyses

For each species (n = 3), the thickness of the cornea was quantified by morphometric analysis using the pre-mentioned software, ImageJ. Three consecutive slides stained by Masson's Trichrome were used, and the absolute thickness of the cornea was calculated by choosing the midpoint (located just in the optical axis). The structures taken into account were the corneal epithelium, Bowman's layer, the corneal stroma, Descemet's membrane and the corneal endothelium. Inter-specific comparisons were made for the relative thickness of this fixed lens. Finally, the focus distance between the cornea and central retina, as well as the curving ray of the cornea, were estimated using a Magnetic Resonance Imaging (MRI) of the medio-frontal plane.

2.7. Magnetic Resonance Imaging

For the Magnetic Resonance Imaging (MRI), each lizard was anaesthetized using an intramuscular injection of Ketamine (20 $mg.kg^{-1}$ body mass, Ketalar® 50 mg/ml). The subject was considered anaesthetized when it lost the ability to push itself back on its feet after being turned on its back and responded weakly to tail pinching. MRI experiments were performed on a 300 MHz (7 T) Bruker Biospec imaging system (Bruker, Ettlingen, Germany) equipped with a Pharmascan horizontal magnet. Ocular globe images for *S. scincus* were acquired with a rapid-acquisition relaxation-enhanced (RARE) imaging protocol using the following parameters: TR/TE = 3000/59.4 ms, RARE factor = 4, NEX = 8, matrix = 256 × 256, FOV = 2 cm, slice thickness = 1 mm, 20 coronal slices, spatial resolution = 79 µm, TA = 25 min 36 s. The parameters for *E. schneideri* were TR/TE = 3000/60 ms, RARE factor = 4, NEX = 4, matrix = 512 × 512, FOV = 2.5 cm, slice thickness = 1 mm, 20 coronal slices, spatial resolution = 49 µm, TA = 25 min 36 s.

The pictures were used to evaluate the relative proportion of the lens volume when compared to the vitreous body volume. The images obtained were also used to assess the diameter (perpendicular to optical axis) and the thickness (parallel to optical axis) of the lens and the ocular globe. This non-invasive method allowed us to evaluate the *in situ* anatomy and morphology of eyes in both species, following various planes without any potential artefacts provoked by eye fixation.

2.8. Oil droplet characterization

After euthanasia, one supplementary individual by species were

used for oil droplet characterization. The eyes were enucleated and cut to flatten the retina. The retina was surgically cut into a PBS filled cup and was then placed on a glass slide. A drop of PBS was put into the retina which was then coverslipped. Oil droplets in the fresh cut tissues were identified on the basis of their localization inside the photoreceptors at high magnification (Leitz® Orthoplan microscope equipped with Leica® DFT7000 camera). The regions located between the central and the most peripheral retina were chosen to allow examination of oil droplets.

2.9. Statistical analysis

All the statistical analyses were carried out using of the software for statistical computing R (version 3.2.1). In function of their distribution, the quantitative data obtained in this study were submitted to parametric (ANOVA one-way or Student's *t*-test) or non-parametric (Kruskal-Wallis or Wilcoxon) tests with a limit of significance set at $p < 0.05$.

3. Results

3.1. Histology

The retinas of *Scincus scincus* (Fig. 2a-c) and *Eumeces schneideri* (Fig. 2d-f) were stained by Masson's Trichrome, allowing the identification of the different histological structures of the eyes. All pictures were taken of the medio-sagittal section of the ocular globe. For both species of skink, the presence of a typical *conus papillaris* was confirmed in the prolongation of the optic nerve (Fig. 2a, d). This highly vascularized structure emerged inside the vitreous body and was located on the medio-sagittal plan of the eye, but shifted downwards relative to the central optical axis. Adjacent to this *conus papillaris*, the central part of the retina of both species, located just on the optical axis (Fig. 2b, e), lacked fovea but possessed the largest thickness and photoreceptor density of the retina. The photo-sensitive retina clearly exhibited three main layers of cells: the photoreceptor layer (which is the innermost layer), the inner nuclear layer at the mid-level, and the ganglion cell layer at the outermost area. These three "granular" layers were identifiable by the presence of their respective numerous dark purple stained nuclei. The peripheral retina (Fig. 2c, f) was much thinner and exhibited a lower density of nuclei in the same three main layers. As illustrated at high magnification for *S. scincus* (Fig. 3a, b) and for *E. schneideri* (Fig. 3e, f), the tips of the photoreceptor outer segments were surrounded by the retinal pigment epithelium. The standard staining method did not allow the differentiation of the cones and the rods, but it was clear that photoreceptors were thinner and more numerous in the central retina (Fig. 3a, e). On the contrary, the peripheral retina of both species (Fig. 3b, f) exhibited thicker and less numerous photoreceptors. Moreover, most photoreceptors of both skink species exhibited an oil droplet located at the basis of the outer segment. This oil droplet appeared less stained and translucent. This structure was more voluminous in the photoreceptors of the peripheral retina (Fig. 3 b, f). The retina was surrounded by the choroid layer, characterized by a high melanocyte density and the absence of tapetum (Fig. 2e). The external scleral layer was reinforced with hyaline cartilage on the backside of the retina (Fig. 2f), with a ring of lamellar bone around the *ora serrata* and the ciliary body (Fig. 2c). Other important structures of the eyes, like the cornea, iris and lens, were investigated (Fig. 3c-d & g-h). The corneal epithelium in contact with the air was thicker and contained more epithelial cell strata in *E. schneideri* (Fig. 3g) versus *S. scincus* (Fig. 3c). The corneal stroma was also more abundant in *E. schneideri*. The iris posterior epithelium, as well as the anterior myoepithelium (dilatator muscle), were pigmented in both species (Fig. 3d, g, h). However, the melanocyte density in iris stroma was more prevalent in the sandfish (Fig. 3d) compared to the Berber skink (Fig. 3h).

3.2. Oil droplets characterization

The oil droplets identified were similar between *S. scincus* (Fig. 4a) and *E. schneideri* (Fig. 4b). According to what we have observed, two populations of cones are distinguishable. One population of cones exhibits oil droplets with a blue-greenish coloration, in both species. A second population of cones seems to exhibit transparent and colorless oil droplets, also in both species.

3.3. Identification of rods by immunohistochemistry

The identification of rods was performed by immunocytochemical targeting of the rhodopsin contained in the photoreceptors. Both skink species exhibited a reactivity against this protein. The sandfish (Fig. 5a-b) and the Berber skink (Fig. 5c-d) showed a similar pattern of reactivity. Strong immunoreactivity was observed in some scattered cells of the central retina identified as "rod-like photoreceptors" (Fig. 5a, c). In contrast, almost no rod-like photoreceptors were found at the peripheral retina for either species (Fig. 5b, d). The specificity of our antigen Rho4D2(Abcam®) was verified by using mammalian retina of *Rattus norvegicus* as a positive control. Moreover, negative controls were essayed by omitting the primary or secondary antibody, or by the substitution of non-immune serum for the primary antibody. No staining was observed on these sections under these conditions.

3.4. Retinal cells

The density of the photoreceptors assessed for both species by morphometric analysis (Fig. 6A) was significantly different at the intraspecific level, but not at the inter-specific one. For each lizard species, the mean number/0.14 mm^2 of photoreceptors was approximately 30% higher at the central retina level. The mean density of photoreceptors per field was 110 and 76 for *S. scincus* (central and peripheral, respectively), and 107 and 71 for *E. schneideri* (central and peripheral level, respectively). Concerning the mean diameter of the inner segment of photoreceptors (cones and rods included), differences, only intraspecific, were observed in function of the localization, with a significant increase of the size during the displacement from the central area towards the periphery of the retina. As illustrated in Fig. 6b, the mean diameters were 4 and 6.2 μm for *S. scincus* (central and peripheral level, respectively), and 4.1 and 6.4 μm for *E. schneideri* (central and peripheral level, respectively).

Nuclei density in the inner granular layer of the retina (corresponding to bipolar, amacrine and horizontal cells) of both species also showed significant differences between the central versus peripheral retinal area (Fig. 7). The sandfish exhibited a mean of 697 and 287 cells per field (central and peripheral level, respectively) and the Berber skink exhibited 402 and 242 cells per field (central and peripheral level, respectively). In contrast, no significant differences were observed between the two species for the identical retinal areas.

Finally, concerning the ganglion cell densities (Fig. 8), significant differences were observed within each species in function of the retinal area, as well as between both species. The mean numbers of ganglion cells were 120.4 and 58.2 for *S. scincus* (central and peripheral, respectively) and 56.3 and 29 for *E. schneideri* (central and peripheral, respectively). Thus, the retinal ganglion cell layer of *S. scincus* presented approximately twice density versus *E. schneideri*.

The retinal ganglion cells (RGC) collect the visual stimuli perceived by the photoreceptors via intermediate cells (bipolar cells, amacrine cells and horizontal cells) and then transmit action potentials via the optic nerve to the visual areas of the brain. When one retinal ganglion cell receives visual stimuli from a single, or a small number of photoreceptors, this corresponds to a linear connection in the retina, which promotes visual acuity. On the other hand, visual sensitivity is favored when a ganglion cell collects visual stimuli from a large number of photoreceptors corresponding to a pyramidal organization of the retina.

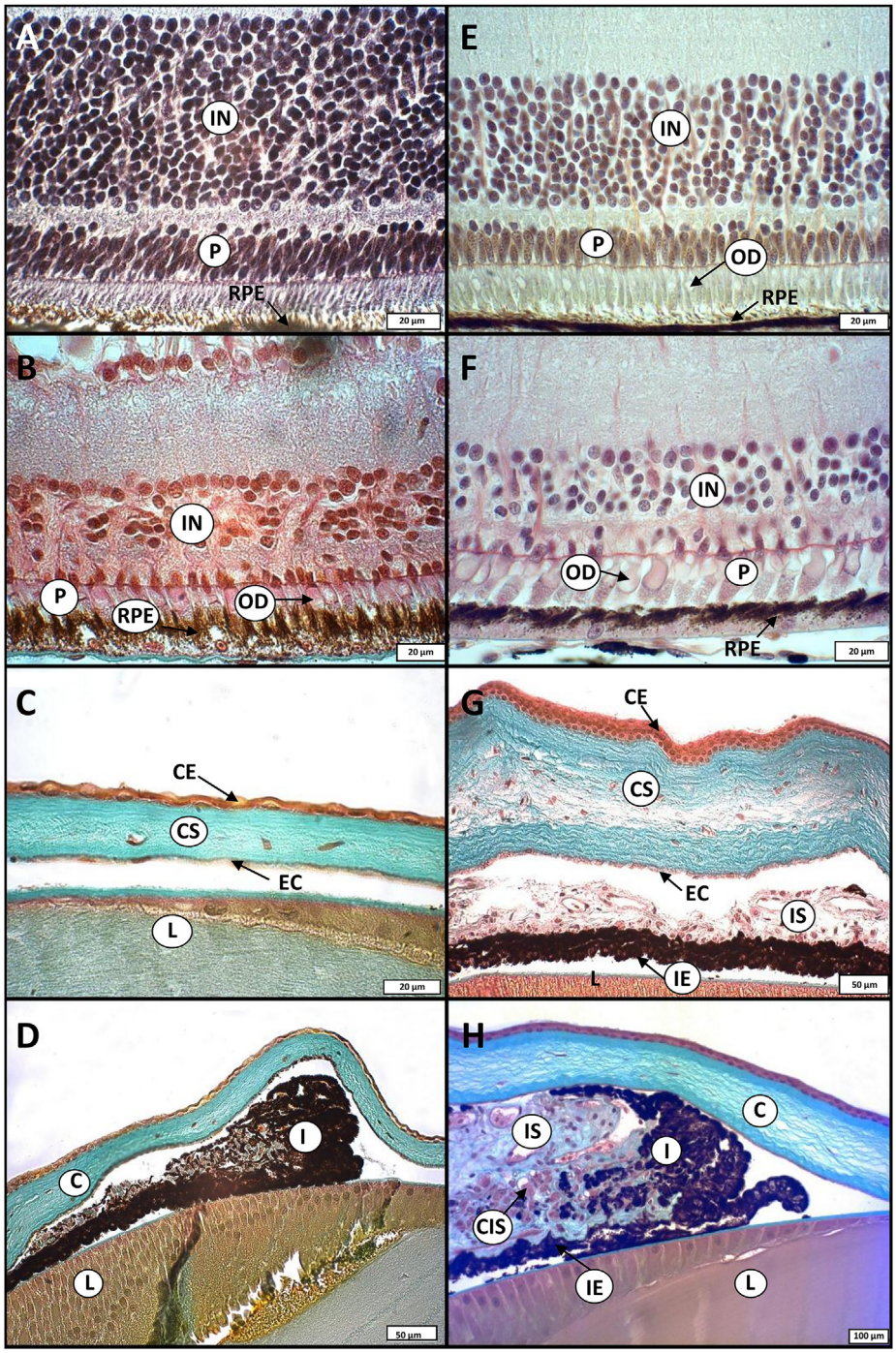

Fig. 3. High magnifications of the eye structures of *S. scincus* (A, B, C, D) and *E. schneideri* (E, F, G, H). Morphological details of the photoreceptor layer in the central (A, E) and peripheral retina (B, F). Pictures illustrating the morphology of the cornea and iris of both species (C, D, G, H). IN: inner nuclear layer (including bipolar, amacrine and horizontal cells), P: photoreceptors, RPE: retinal pigmented epithelium, OD: oil droplets, CE: corneal epithelium, CS: corneal stroma, EC: endothelium of cornea, L: lens, I: iris, C: cornea, IS: iris stroma, IE: iris anterior myoepithelium (dilatator muscle) and posterior epithelium, CIS muscles of circular iris sphincter.

In order to estimate how neurons are connected inside the retina (linear or pyramidal organization), we calculated the ratio between the photoreceptor cells of the base and the ganglion cells collecting the signal from, and transmitting information to, the brain (Fig. 9). In both species, this ratio differed in function of the retinal localization (central versus peripheral). The ratio (ganglion cell number/photoreceptor number) decreased from the center to the periphery, indicating a shift from a linear connection to a more pyramidal pattern when we move away from the central retina. More interestingly, Fig. 9 highlights an inter-specific significant difference between the ratios recorded in the central retina. Indeed, the mean ratios were 1.09 for *S. scincus* versus 0.52 for *E. schneideri*, pointing to a more linear connection in *S. scincus*, whereas the Berber skink showed a more pyramidal organization.

3.5. Respective density of rods and cones

Immunohistochemistry was performed with anti-rhodopsin antibodies elicited to distinguish cones (unstained) from rods (labeled in brown). Morphometric analysis of cone densities pointed to significant differences between central and peripheral retinal areas for both species

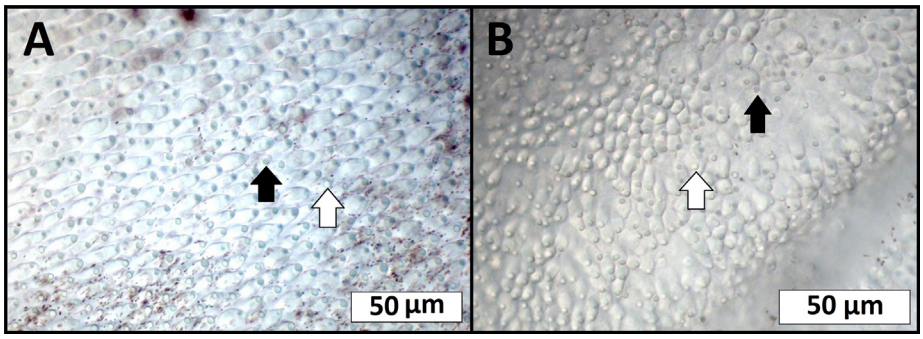

Fig. 4. Histological photographs of the cones containing oil droplets of *S. scincus* (A) and *E. schneideri* (B). The black arrows indicate the pale blue-greenish oil droplets whereas the white arrows indicate the transparent colorless oil droplets associated to two cones populations. (For interpretation of the references to color in this figure legend, the reader is referred to the web version of this article.)

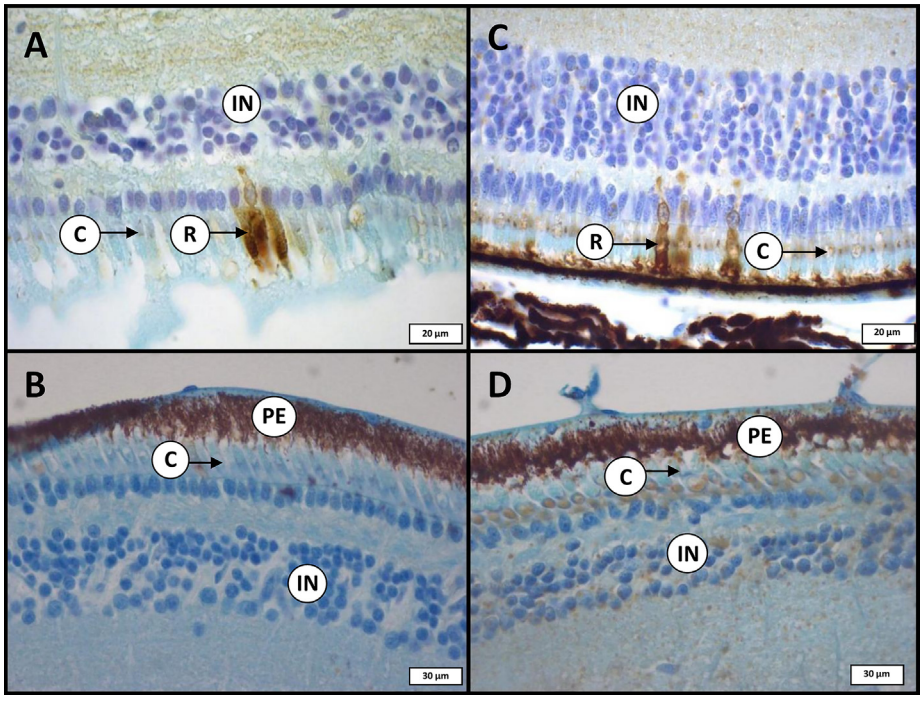

Fig. 5. Immunohistochemical detection of rhodopsin in retinal cells of *S. scincus* (A, B) and *E. schneideri* (C, D). Photographs of the central (A, C) and peripheral (B, D) retinal areas. PE: pigmented epithelium, IN: inner nuclear cell layer (including bipolar, amacrine and horizontal cells), C: cones (rhodopsin-negative photoreceptors), R: rod-like cells (rhodopsin-positive photoreceptors).

(Fig. 10a), which was in agreement with the pre-mentioned global photoreceptor counting. The mean numbers of cones/0.22 mm^2 for *S. scincus* were 45.7 and 28.27 (central and peripheral, respectively), and 47.2 and 25.93 for *E. schneideri* (central and peripheral, respectively). In contrast, the rod densities were significantly lower in both species, but showed the same intra-specific differences between the central versus peripheral retinal areas (Fig. 10b). The mean numbers of rods for *S. scincus* were 1.86 and 0.03 (central and peripheral, respectively), and 1.1 and 0.21 for *E. schneideri* (central and peripheral, respectively). No inter-specific differences were evidenced for either cone nor rod densities.

The ratio of photoreceptors (rods/cones), presented in a boxplot in Fig. 11, gives a view of the retinal composition. The pattern logically follows the same intra-specific differences previously mentioned, with a high domination of cones in both species and their retinal areas. The mean ratios for *S. scincus* were 0.05 and 0.001 (central and peripheral, respectively), and 0.025 and 0.006 for *E. schneideri* (central and peripheral, respectively). We can note that the mean ratio for the central retina of the sandfish was approximately twice that of the Berber skink, but this tendency was not statistically significant.

3.6. Cornea morphometric analyses

The absolute thickness of the cornea, estimated using morphometric software, was significantly different between our two species of skinks (Fig. 12). The mean thickness was about 36.88 µm for *S. scincus* and about 109.68 µm for *E. schneideri*.

3.7. Ocular geometry and topography analyzed by MRI

The images obtained by MRI (Fig. 13), were used to obtain precise dimensions of the eyes' optical parameters in the live animals. Three main structures of the ocular globes were analyzed: the cornea, the vitreous body and the lens. The images were T2-weighted so the more aqueous, like the vitreous body, structures appeared light grey, whereas the harder structures, like the lens, appeared in black. Beneath the ocular globes, the bottom half of each image was mostly occupied by the muscular tongue.

The principal geometrical values (total axial length, maximal diameter, corneal radius of curvature, lens length and diameter, length from nodal point to central retina, relative lens diameter, lens flattening ratio) are summarized in Table 1.

In sandfish (Fig. 13a), the eyeballs occupy a large part of the cranial volume and the interorbital space is very small. On the other hand, in the Berber skink (Fig. 13b) the space occupied by the eyes within the cranial volume is smaller, and the internal separation zone between the two eyeballs is larger. In both species, the eyes are not spherical, but adopt a flattened bell-shaped structure with a significant protrusion of the cornea and lens at the anterior face of the eyeball. The gross anatomical size of the eyes of both species was estimated by measuring the

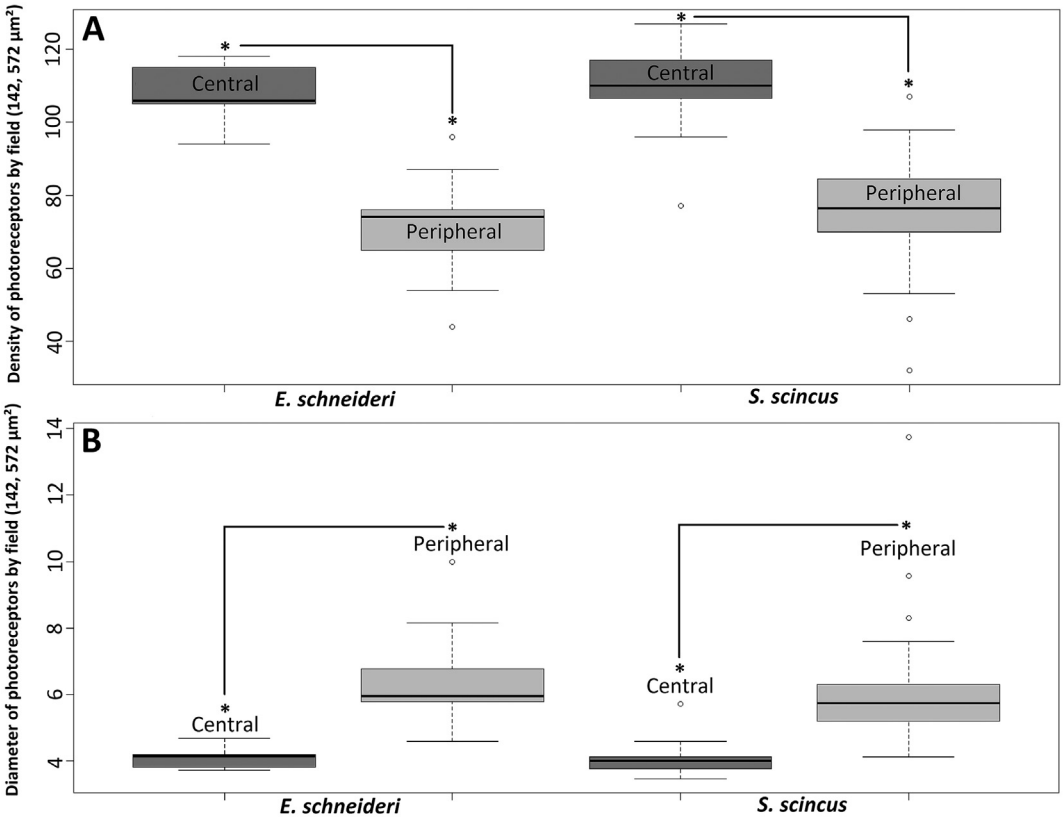

Fig. 6. (A) Boxplots representing the density of photoreceptors (number of nuclei in external nuclear layer/microscopic field of 142, 572 µm^2) of both *S. scincus* and *E. schneideri,* in the central and peripheral retinal zones. Data were analyzed by the non-parametric Kruskal-Wallis test and significant differences set at p-value < 0.05. (B) Boxplots representing the diameter values in µm (at the level of the outer segment) of photoreceptor cells of both *S. scincus* and *E. schneideri*, in the central and peripheral zones. Data were analyzed by the non-parametric Kruskal-Wallis test and significant differences set at p-value < 0.05.

ratio (length /equatorial diameter) of the eyeball (Fig. 15a). We have shown that the eyes of the sandfish are slightly more spherical than those of the Berber skink, the ratio being of 0.85 for the former, and 0.80 for the latter.

The percentage values obtained for the relative proportions of the vitreous body surfaces were significantly different between the two species (Fig. 14). The mean values were 80.45% for *S. scincus* versus 72.40% for *E. schneideri*. The vitreous body, therefore, seemingly occupies more volume for the sandfish (the scanned surface in coronal view giving a good approximation of the volume). Logically, the relative volume occupied by the lens is inverted, with the mean percentage of scanned lens surface being 19.54% for *S. scincus* and 27.6% for *E. schneideri,* and this difference was also significant. Moreover, the sphericity of the lens was significantly less for *S. scincus* than for *E. schneideri*, the ratio (thickness/diameter) being of 0.66 for the former and of 0.76 for the latter (Fig. 15b).

4. Discussion

The histological observations in light microscopy provided useful information about the general retinal morphology of both species. The presence of a conus papillaris rising into the vitreous has been confirmed. This highly vascularized structure observed in lizard eyes is considered as a homologue of the pectin oculi of birds (Braekevelt, 1989). The function of retinal nutrition and oxygenation, attributed to this structure, remains the subject of hypotheses, including a plausible

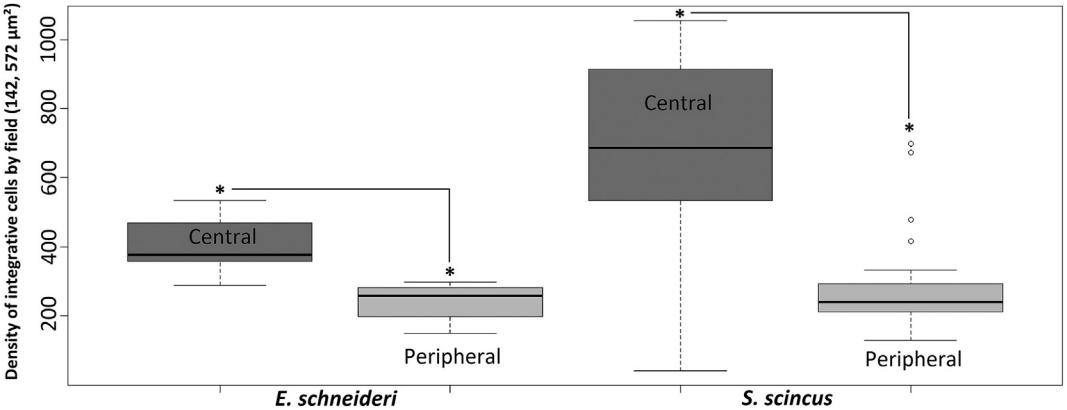

Fig. 7. Boxplots illustrating the density of integrative cells (number of nuclei in internal nuclear layer/microscopic field of 142, 572 µm^2) of both *S. scincus* and *E. schneideri,* in the central and peripheral retinal areas. Data were analyzed by the non-parametric Kruskal-Wallis test and significant differences set at p-value < 0.05.

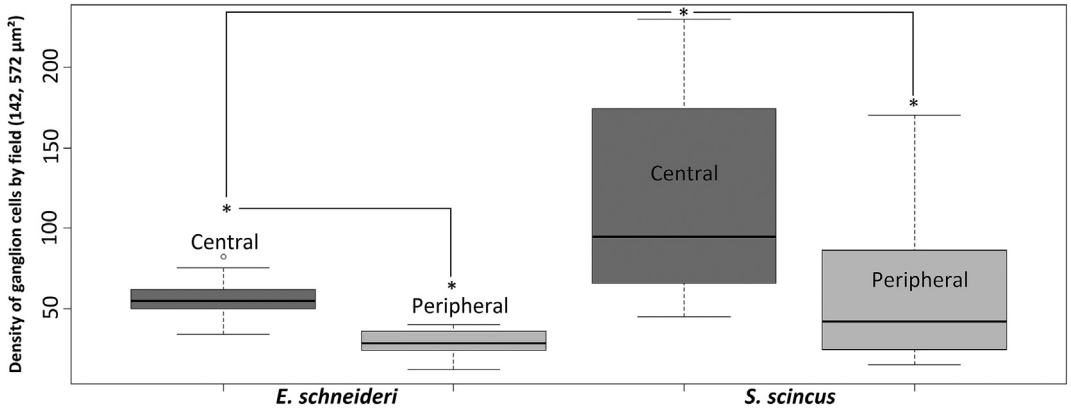

Fig. 8. Boxplots representing the density of ganglion cells (number of nuclei in ganglion cells layer/microscopic field of 142, 572 µm^2) of both *S. scincus* and *E. schneideri,* in the central and peripheral retinal zones. Data were analyzed by the non-parametric Kruskal-Wallis test and significant differences set at p-value < 0.05.

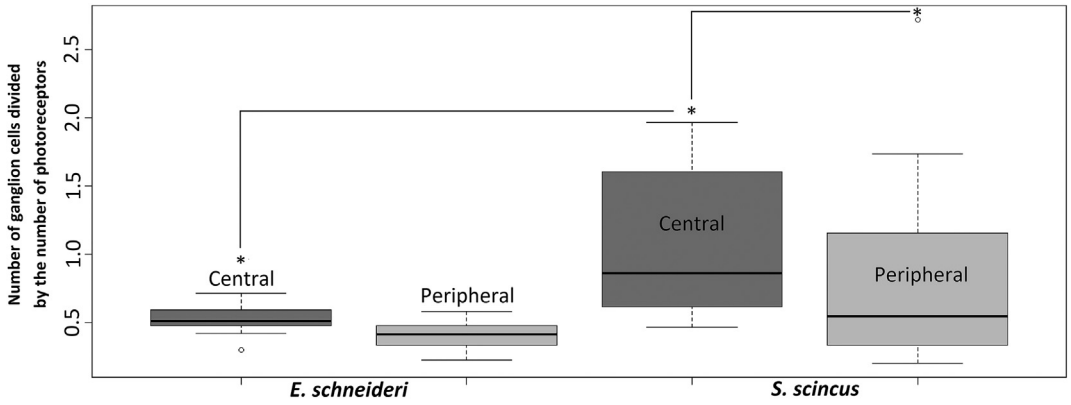

Fig. 9. Boxplots representing the ratio (number of ganglion cells/number of photoreceptors) calculated in the central and peripheral retinal areas of *S. scincus* and *E. schneideri,* respectively. Data were analyzed by the non-parametric Kruskal-Wallis test and significant differences set at p-value < 0.05.

link to scotopic vision, leading potentially to a less developed structure, as observed in snakes. This, however, has yet to be clarified (Dieterich, Dieterich, & Hildebrand, 1976; Walls, 1942). In contrast to the conus papillaris, no fovea were found in either of the studied species of skinks. These results seem congruent with the literature on Scincidae (New et al., 2012; Zhao et al., 2019). Single fovea, characterized by a conical depression of the retina in the optical axis and a very high density of cone receptors, are present in numerous Squamata families, such as Agamidae (Barbour et al., 2002; Detwiler & Laurens, 1920). The lizards of the genus *Anolis* also possess a double fovea (central and lateral) (Fite & Lister, 1981; Makaretz & Levine, 1980), such as those observed in diurnal raptorial birds (Jones, Pierce, & Ward, 2007; Ruggeri et al., 2010). Despite the absence of fovea, the central retina of *S. scincus* and *E. schneideri* are characterized by a high density of photoreceptors compared to peripheral retina.

The retinal photoreceptor typesetting of *S. scincus* and *E. schneideri* appeared to be mainly dominated by cones, the ratio at the central retina ranging from 20 to 40 cones for only one rod (ratio range 0.05–0.025). This observation is in accordance with other studies indicating that most families of lizards possess a retina exclusively constituted of cones. The rare studies focusing on the retinal structure in Scincidae also point to a pure cone retina or one largely dominated by cones. In the case of the species *Cryptoblepharus boutonii* (Röll, 2001b), for example, the retina is entirely composed of cones, both single and double. On the other hand, the Australian species *Tiliqua rugosa* seems to have a mixed retina with a ratio of cones-rods equal to 80:1 (Braekevelt, 1989). A recent, and fascinating study, by Zhao et al. (2019) brought new insights to the field of the retinal histology of Scincidae. This study showed that three other species of skink, *Acontias orientalis*, *Acontias rieppeli* and *Trachylepis punctatissima*, also have a pure cone retina. It is, however, important to say that the characterization of the photoreceptors in the abovementioned study was only based on morphological parameters. In contrast, our study is based on the immunohistochemical detection of rhodopsin, a protein found specifically in rods. Therefore, we should also be cautious about a firm classification of photoreceptors. Indeed, the literature now clearly shows that both ultrastructural and molecular criteria are needed to fully describe a photoreceptor and to attribute its type without ambiguity. For example, the photoreceptors of nocturnal geckos are cones, as it is the case with their diurnal ancestors (Taniguchi, Hisatomi, Yoshida, & Tokunaga, 1999). This conclusion is not only attested regarding the opsins that they use, but even by morphological and ultrastructural criteria, as shown in detail in the study of Röll (2000). Moreover, in a recent study (Bhattacharyya, Darren, Schott, Tropepe, & Chang, 2017), it has been shown that the snake species *Pituophis melanoleucus* has cones containing rhodopsin. Schott et al. (2016) obtained similar results in another Colubridae species (*Thamnophis proximus*). Both of these studies support this opposite transmutation pattern, leading to a switch from rods to cones within these snakes. We should then be open to the fact that photoreceptors with intermediate features (for example, exhibiting cone morphology but biochemical rod characteristics) could be found in some peculiar species, including the psammophilic lizards described in the present article. For these reasons, it is more adequate to speak about “rod-like” photoreceptors when referring to the rhodopsin expressing photoreceptors found in *S. scincus* and *E. schneideri*. Although it is necessary to remain cautious, our results strongly suggest that the two species of psammophilic skinks described in the present study have a duplex retina containing both rods and cones. Reinforcing

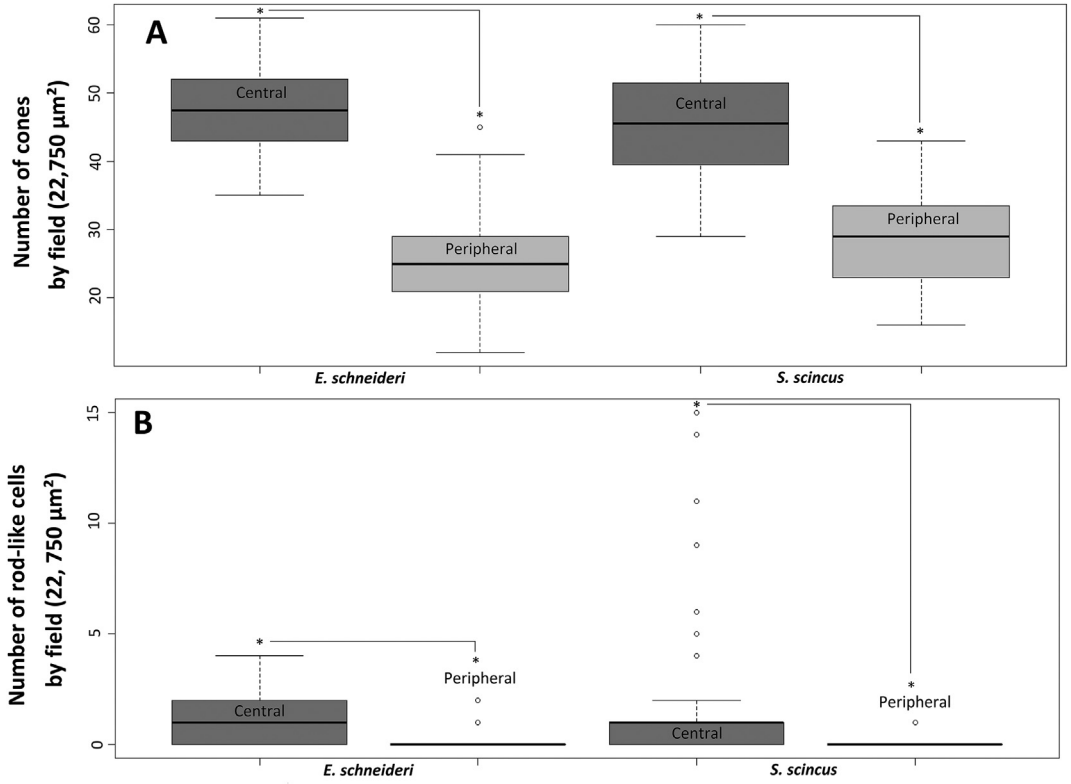

Fig. 10. Boxplots representing the number of cones (A) and "rod-like" cells (B) by microscopic field of 22, 750 µm^2 in the central and peripheral retinal zones of *S. scincus* and *E. schneideri*, respectively. Data were analyzed by the parametric ANOVA one-way test and significant differences set at p-value < 0.05(A) or by the non-parametric Kruskal-Wallis test and significant differences set at p-value < 0.05(B).

this hypothesis, the study of New et al. (2012), performed on the skink species *Tiliqua rugosa*, also highlighted a subset of photoreceptors that were immunoreactive to rhodopsin. As noted in this paper, this is not the first time that photoreceptors expressing rhodopsin were identified in Squamata, as shown in the species *Chamaeleo chamaeleon* (Bennis et al., 2005). Additionally, and again to reinforce our results, a study of Khattab et al. (2004) performed on various reptiles, including *E. schneideri*, showed that the retina of this species contains morphologically identifiable rods. These photoreceptors, of which only a small amount are present, were studied by transmission electron microscopy (TEM), and the rods were identifiable thanks to their smaller inner segments (Khattab et al., 2004). Finally, we have evidenced, using light microscopy, the presence of oil-droplets in the cones of both skink species. These spherical lipidic inclusions found in the inner segment of the cones are really interesting considering the fact that they play an important role. Indeed, they focus incident light thanks to their being shaped like a spherical lens (Wilby & Roberts, 2017). The two identified populations of cones observed in both skink species have never been described before. According to the literature, the presence of, at least, two kind of oil droplets indicates that the visual capacities of these two psammophilic species could be complex. The pale blue-greenish oil droplets probably serve as filters (Stavenga & Wilts, 2014) whereas the colorless ones act as a micro-lens (Wilby & Roberts, 2017). The similarity between the two species could indicate similar adaptive answers to their light environment. As reminded by the study of Yovanovich (2019), the presence and coloration of oil droplets is associated with lifestyle in vertebrates. Similarly with the fossorial species *C. nicterus*, both species of skinks exhibit colorless oil droplets which are probably used to improve light detection (Yovanovich et al., 2019). The presence of at least one type of colored oil droplets could be an indication that

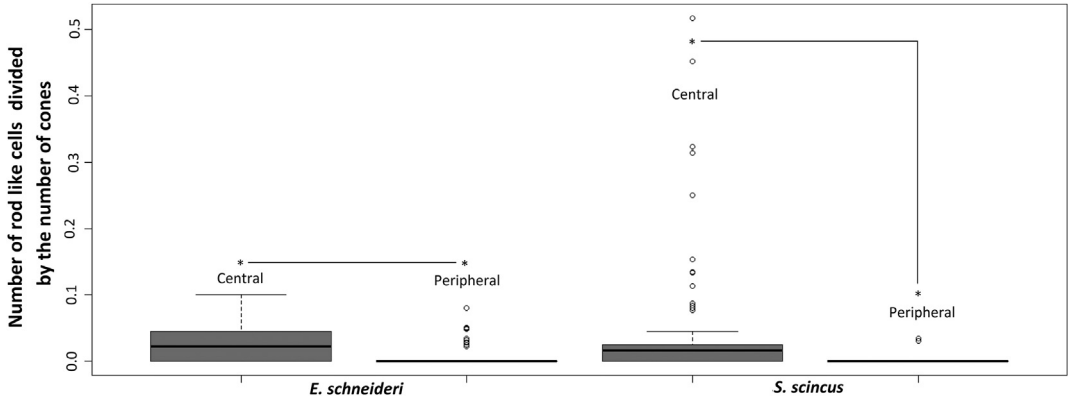

Fig. 11. Boxplots representing the ratio (number of "rod-like" cells/number of cones) calculated in the central and peripheral retinal areas of both species (*S. scincus* and *E. schneideri*). Data were analyzed by the non-parametric Kruskal-Wallis test and significant differences set at p-value < 0.05.

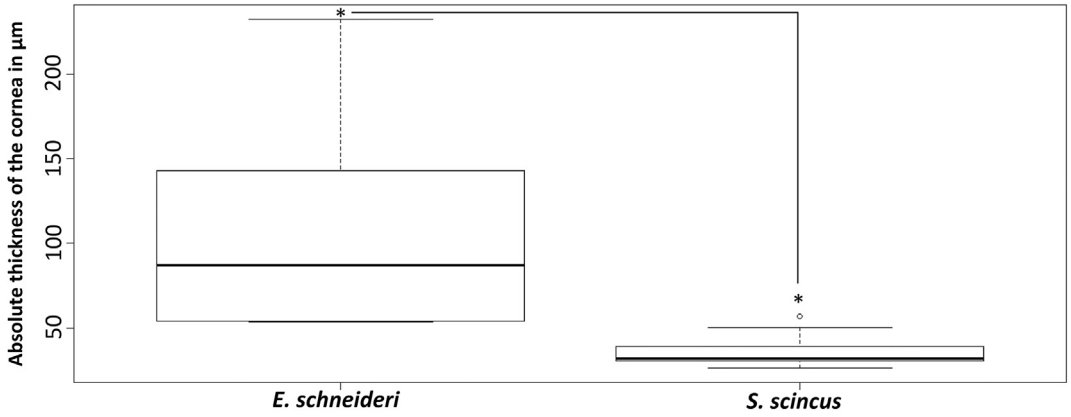

Fig. 12. Boxplots representing the absolute thickness of cornea measured on three microscopic fields/ animal picked at random in the central part of cornea of both *S. scincus* (n = 3) and *E. schneideri* (n = 3). Data were analyzed by a Wilcoxon test and significant differences set at p-value < 0.05.

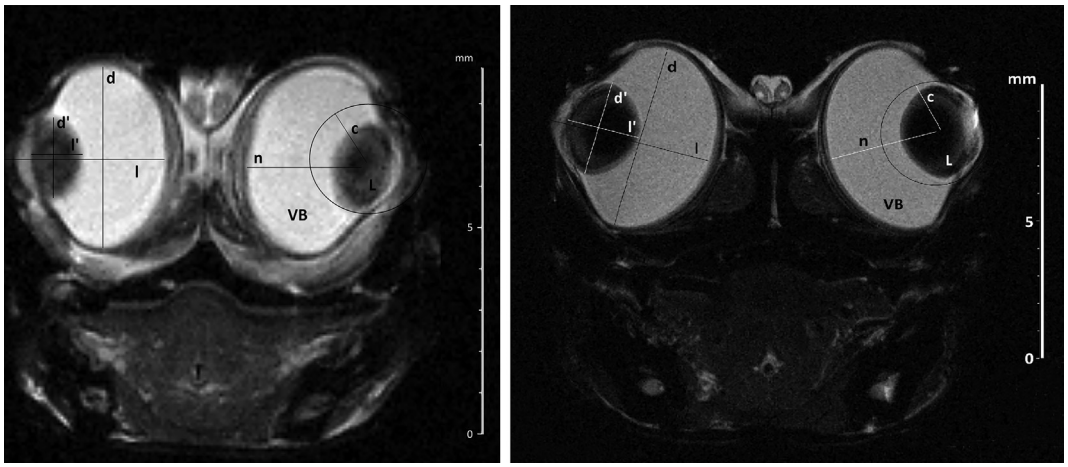

Fig. 13. (A): MRI transverse plane view of *S. scincus* head showing the large occupation of ocular globes, (B): comparable transverse image of *E. schneideri* head showing the eyeballs. d: ocular globe maximal diameter, d': lens diameter, l: total axial length, l': lens length (thickness), n: length from nodal point to central retina, c: corneal radius of curvature, VB: vitreous body, L: lens. The scale on the right of each image is in millimeters.

both species are exposed, at least partially, to high light intensity.

Another part of the retina, the retinal ganglion cells (RGC), are a relevant and interesting feature. As noted in the study of Malkemper and Peichl (2018), the density of RGC is used as a tool to assess the visual acuity of species independently of the presence or absence of fovea. The number of both rods and cones exceed the number of ganglion cells, creating a bottle-neck to transmit the neurological signals. The density and absolute number of ganglion cells is an indirect indication of visual acuity. The mathematical models of anatomical spatial resolution use the density of RGC, which is usually measured in retinal wholemounts, and the focal length (posterior nodal distance) of the eye (Land & Nilsson, 2012). The visual acuity in vertebrates is highly dependent on the photoreceptor density and the types of connections made to ganglion cells via bipolar cells. In humans and other primates, the central part of fovea contains, as a mean, one cone connected to a single bipolar cell, which is itself connected to a single ganglion cell. This results in a 1:1 ratio of cones to ganglion cells. This linear direct connection provides the anatomical basis for high acuity (Boycott & Wassle, 1999; Kolb & Dekorver, 1991; Kolb & Marshak, 2003). In contrast, in the peripheral primate retina the number of photoreceptors (cones or rods) converging onto a single ganglion cell increases, so that the ratio (ganglion cells/photoreceptors) decreases from 1:5 in the macula lutea surrounding fovea to 1:100 in very peripheral zones of retina. This pyramidal connection pattern correlates with decreased peripheral acuity (Boycott & Wassle, 1999; Polyak, 1941) but promotes retinal sensitivity in scotopic conditions. A similar observation was noted in some bird species, such as the pigeon (*Columba livia*) (Querubin, Lee, Provis, & Bumsted O'Brien, 2009). In both species *S. scincus* and *E. schneideri,* the ratio (ganglion cells/photoreceptors) in the central retina is quite equal to 1:1, suggesting a good acuity. This ratio decreases to 1:2–1:3 in peripheral retina, but remains low, indicating a pyramidal tendency but with a very small base. This observation suggests that acuity remains high, including in peripheral area. In contrast we could suspect that the sensitivity in scotopic condition is not favored by this pattern of retinal cell connections.

In addition to the retinal structure and composition, the overall shape of the ocular globe gives useful information about the visual ecology of a species (Hall & Ross, 2007). As has been shown for birds, the overall shape is linked to the activity pattern of a species. Birds that are adapted to scotopic vision have a larger corneal diameter relative to the axial length. On the contrary, phototopic species of birds have a longer axial length, optimizing the visual acuity. The same results are found among reptiles, like the study of Hall (2008) performed on 116 lizard species brilliantly shows. The results that we have obtained from the MRI show that the eyes of *S. scincus* are more spherical than those of *E. schneideri* that show a flattened bell-shaped form. We may infer that the sandfish therefore has a slightly more photopic pattern. Moreover, the lens shape is flatter in *S. scincus* versus *E. schneideri*. The lens plays an important role for the vision of vertebrates, focusing the incident light on the retina (Land, 2012). There is a common link between the pupils' shape and the lens' optical properties (Malmström & Kröger, 2006). Indeed, vertebrate species may exhibit either slit pupils,

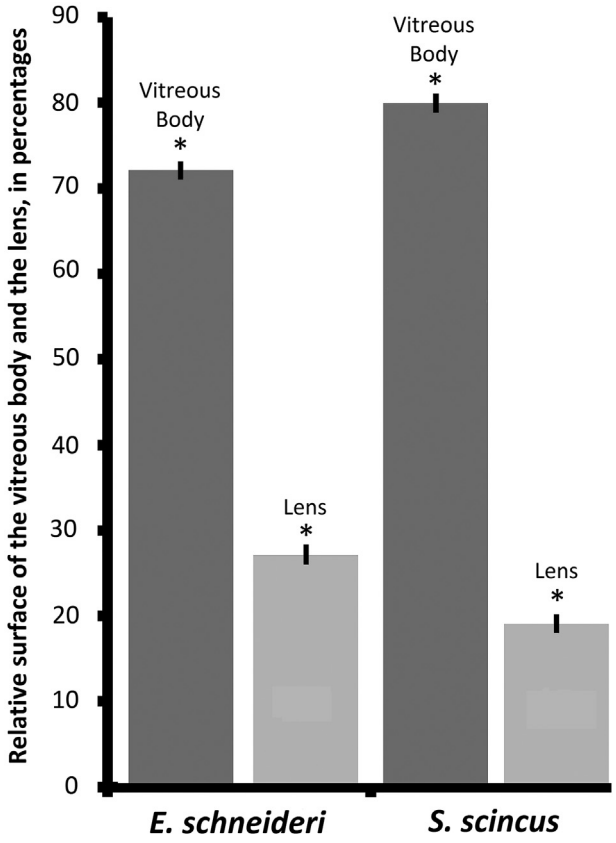

Fig. 14. For each species (*S. scincus* and *E. schneideri*), histograms illustrated the mean relative surface (in %) occupied inside ocular globe by the vitreous body and the lens, respectively. The surfaces were evaluated on RMI images taken in medio-sagittal plane of eyes. Mean values ± SD recorded in each species were compared by an ANOVA one-way test and significant differences set at p-value < 0.05.

Table 1
Mean values (± Standard Deviation) of the mentioned principal geometrical values of *S. scincus* (n = 3) and *E. schneideri* (n = 3). All the values are in millimeters except for the last two ratios. The "relative lens diameter" corresponds to the ratio (diameter of the lens versus global diameter of the eye) and the "lens flattening ratio" corresponds to the ratio (the thickness of the lens versus its diameter). These values are presented as (mean ratio ± relative SD) which are without units. All the parameters are statistically different between the two species. Data were analyzed by Student's *t*-test (except for the lens length analyzed by a Wilcoxon test) and significant differences set at p-value < 0.05.

Principal geometric values	*S. scinus*	*E. schneideri*	Student's *t*-test analysis
Total axial length	3.85 ± 0.11	5.28 t 0.15	p < 0.05
Maximal diameter	4.53 ± 0.13	6.59 ± 0.04	p < 0.05
Corneal radius of curvature	1.36 ± 0.04	1.91 ± 0.09	p < 0.05
Lens length	1.28 ± 0.14	2.56 ± 0.14	p < 0.05
Lens diameter	1.93 ± 0.13	3.37 ± 0.07	p < 0.05
Length from nodal point to central retina	2.79 ± 0.14	3.77 ± 0.12	p < 0.05
Relative Lens diameter	0.42 ± 0.03	0.51 ± 0.01	p < 0.05
Lens flattening ratio	0.66 ± 0.03	0.76 ± 0.02	p < 0.05

associated with multifocal lenses while round pupils could be associates with monofocal or multifocal lenses. Both of our species of skink present, broadly speaking, round pupils therefore we can deduce nothing from the presence of monofocal or multifocal lenses in these species. However, it would be interesting to determine whether these two skink species have a monofocal or multifocal lenses. This could be assessed by a refractometry method as described by Malmström and Kröger (2006). It is interesting to add that the ratio (diameter of the lens versus global diameter of the eye) called in the Table 1 and in the following section "relative lens diameter" can give an indication about the ocular specialization and performance. For example, truly diurnal species, as Simians and Psittacidae, possess a relative lens diameter of 0.3–0.4, whereas nocturnal animals such as opossum and galago have one ranging from 0.6 to 0.8 (Land, 2012). The species which are active as well as during day and night, such as Equidae and numerous mammalian carnivores, have a relative lens diameter of about 0.4–0.5 times the diameter of the eye itself (Land, 2012). In both skinks these ratios ranged from 0.4 (*S. scincus*) to 0.5 (*E. schneideri*). These results combined to proportion of photoreceptors (cones and rods) in retina suggest that these two species have a mainly photopic vision based on the activity of cones but could also have a functional vision in lowest light intensities as crepuscular conditions. The presence of a small population of rods in the retina of these species and the morphology of the outer segments of cones showing that they are quite small and thus don't suggest a high light sensitivity, enhances this hypothesis. These lizards could be active at dusk corresponding to mesopic vision in which both photoreceptor types are functional. However, the absence of observations of these two species under natural conditions studying their periods of activity relative to the light intensity does not allow to confirm this hypothesis.

On the other hand, the study of Schachar, Pierscionek, and Le (2007) showed that vertebrate species exhibiting a flattened lens ratio (expressed here as the central lens thickness divided by equatorial lens diameter), lower or equal to 0.6, have a high accommodation amplitude, as is the case for primates, diving birds and diurnal birds of prey. The high "lens flattening ratio" values (0.66 in *S. scincus* and 0.76 in *E. schneideri*) that we have estimated in the present study point to a tendency to have a spherical lens shape and could thus be an indication that both psammophilic skinks have low accommodation capacities, close to those of owls and most mammals (possessing thick lenses).

The cornea is the major refractive element of the eye and therefore plays a key role in focusing the light on the retina. The cornea is significantly thicker in *E. schneideri* compared to *S. scincus*, indicating that the number of diopters provided by the cornea is greater in *E. schneideri* versus *S. scincus*. The number of diopters provided by the cornea depends on the relative size of the eye which is proportionally smaller in *E. schneideri* versus *S. scincus* compared to the respective sizes of the animals. It also depends on the power of accommodation of the lens since both structures (cornea and lens) are involved in focusing the light rays on the retina. It is possible that the power of accommodation is less effective in *E. schneideri* (compared to *S. scincus*) which would require, to compensate, to have a thicker cornea giving a higher number of diopters. However, these considerations remain highly speculative and go far beyond the scope of this work.

Moreover, in reason of its position open on the outside, this structure of eyeball is the most vulnerable to external influences as pathogens or erosion induced by abrasive particles. Indeed, the cornea has the main role of protecting the eye from external damage caused by the environment (Koudouna et al., 2018). The corneal epithelium is finer in *S. scincus* (3 strata) than in *E. schneideri* (5–6 cell layers), suggesting better protection against abrasion in this last species. It is possible that the Berber skink moving, with open-eyes, on the sand surface is more exposed to sandstorm and abrasion than the sandfish, which is buried most of the time and whose eyes are likely to be protected by closed eyelids when *S. scincus* sojourns inside the substrate. However, to confirm this speculative hypothesis, it would be important to study if the eyelids (including the nictitating membrane) are open or closed during the time when the animal is buried in the sand.

Finally, a very recent paper, similar to our study, highlighted the functional anatomy of the eyes of a neotropical fossorial lizard (Yovanovich et al., 2019). This fossorial species, *Calyptommatus nicterus*, belonging to the Scincomorpha (Gymnophthalmidae), shares

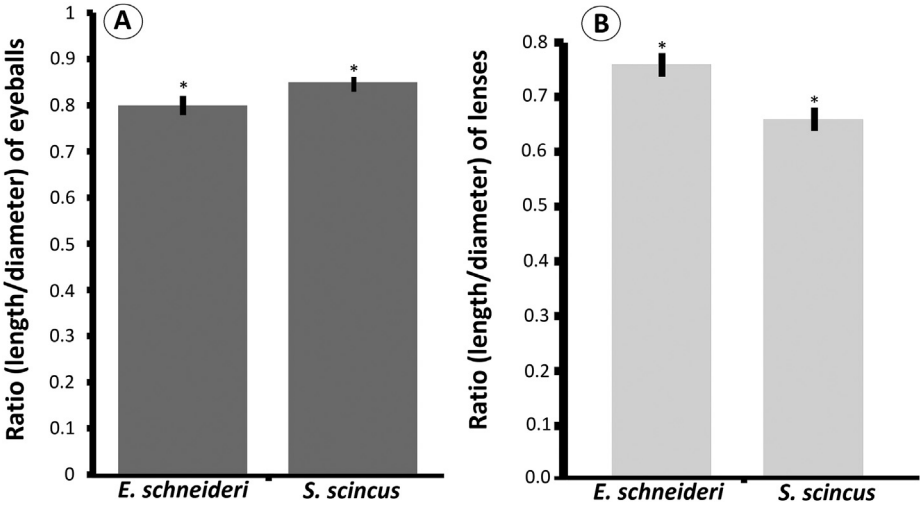

Fig. 15. (A) Histograms representing the ratio between the length (following optical axis) and the maximal transverse (equatorial) diameter of the ocular globe for both species. Mean values ± SD recorded in each species were compared by Student's *t*-test and significant differences set at p-value < 0.05. (B) Histograms representing the ratio between the length (thickness) and the diameter of the lens for both species. Mean values ± SD recorded in each species were compared by Student's *t*-test and significant differences set at p-value < 0.05.

many features with our two model species. More precisely, *C. nicterus* lives in sandy continental dunes, composed of loose sand, possesses a short tail with an elongated body, and is buried in the sand most of the time (which makes it closer to *S. scincus*). This species exhibits many cones with colorless oil-droplets and highly transmissive lenses but the data of this study could not exclude the presence of rods in retina. This study challenges the general assumption that fossorial species undergo a loss of visual capacity, an affirmation generally based on the reduced size of the eyes in these species. Yovanovich and collaborators conclude that, the visual system of *C. nicterus* is well adapted for vision in bright light and presents some cytological specializations as colorless oil-droplets that improve sensitivity in dim light, suggesting that this fossorial lizard might perform some visually-dependent behaviour above the surface of open dune when light levels are relatively high. We could draw a similar conclusion with regard to the results of the present study. Indeed, beside the fact that *S. scincus* & *E. schneideri* have different lifestyles, with the sandfish living most of the time buried in the sand, it exhibits similar visual capacities with its sister species. Moreover, the very similar retina between the two species excludes a strict loss of visual capacities that could have been hypothesized, with, for example, a reduced size of the eyes or a low density of photoreceptors in central retina or a pyramidal organization of retinal connections which is by no means the case. The absence of fovea, and the rather spherical lenses are also shared features that reinforce the similarity between these two skinks. It would, nevertheless, be interesting to investigate the role played by the visual perception of prey by *S. scincus* during hunting, even though this species is known to use vibratory cues to detect insects on the surface of the sand (Hetherington, 1989). However, the study of Attum et al. (2004) demonstrates that *S. scincus* is an opportunistic feeder and dietary generalist. Indeed, the diet of *S. scincus* is far from being strictly insectivorous. This species also consumes numerous plants in the form of seeds or leaves. In the aeolian deserts, plants are rare forcing many reptile species to consume plant debris and anemophily seeds carried by the wind (Arnold, 1984; Pietruszka, Hanrahan, Mitchell, & Seely, 1986; Robinson & Cunningham, 1978). These windblown plant debris are an important food source in aeolian sand deserts (Seely, 1991). The sandfish *S. scincus* follows this trend, indeed individuals were observed consuming windblown seeds and dried leaves, on the crests of sand dunes. These vegetal detritus and seeds were not detected by vibration but well by visual screening during diurnal period requiring an efficient visual system in photopic conditions. To our knowledge, no study mentions the eating behavior of *E. schneideri* in natural conditions. But in captivity it is known that it locates its food (insects or vegetables) visually on the surface of sand under a significant light intensity requiring also a good visual acuity.

Author contributions

J. Canei: Conceptualization, Investigation, Data curation, Formal analysis, Methodology & Writing - original draft. **C. Burtea:** Methodology, Validation & Supervision. **D. Nonclercq:** Conceptualization, Investigation, Funding acquisition, Methodology, Project administration, Supervision, Validation, Writing - review & editing.

Declaration of Competing Interest

The authors declare that they have no known competing financial interests or personal relationships that could have appeared to influence the work reported in this paper.

Acknowledgments

Jérôme Canei is the recipient of a fellowship from ARC (Actions de Recherche Concertée) of the French Community of Belgium. The expert technical assistance of Mrs Françoise Coulon and Giuseppina Ninfa was greatly appreciated. The manuscript reading by Natalie Dickson (Service of Proofreading and Translation, University of Mons) was gratefully acknowledged. We also greatly thank Sarah Hennuy and Jérôme Francq from the Animal House Facility of the University of Mons.

References

Allam, A. A., Abo-Eleneen, R. E., & Othman, S. I. (2017). Microstructure of scales in selected lizard species. *Saudi Journal of Biological Sciences, 26*(1), 129–136.
Ammermüller, J., Muller, J. F., & Kolb, H. (1995). The organization of turtle inner retina. II. Analysis of color-coded and directionally selective cells. *Journal of Comparative Neurology, 358*(1), 35–62.
Arnold, E. N., & Leviton, A. E. (1977). A revision of the lizard genus *Scincus* (Reptilia : Scincidae). *Bulletin of the British Museum Natural History Zoology, 31*(5).
Arnold, E. N. (1984). Ecology of lowland lizards in the eastern United Arab Emirates. *Journal of Zoology London, 204*, 329–354.
Attum, O., Covell, C., & Eason, P. (2004). The comparative diet of three Saharan sand dune skinks. *African Journal of Herpetology, 53*(1), 91–94.
Ayaz, D., Çiçek, K., Tok, C. V., & Dinçaslan, Y. E. (2011). A new record of Eumeces schneideri (Daudin 1802 in Northeastern Anatolia, Turkey. *Biharean Biologist, 5*(1), 78–79.
Barbour, H. R., Archer, M. A., Hart, N. S., Thomas, N., Dunlop, S. A., Beazley, L. D., & Shand, J. (2002). Retinal characteristics of the ornate dragon lizard, *Ctenophorus ornatus*. *Journal of Comparative Neurology, 450*(4), 334–344.
Baumgartner, W., Fidler, F., Weth, A., Habbecke, M., Jakob, P., Butenweg, C., & Böhme, W. (2008). Investigating the locomotion of the sandfish in desert sand using NMR imaging. *PLoS ONE, 3*(10), e3309.
Bennis, M., Molday, R. S., Versaux-Botteri, C., Repérant, J., Jeanny, J.-C., & McDevitt, D. S. (2005). Rhodopsin-like immunoreactivity in the 'all cone' retina of the chameleon (*Chameleo chameleo*). *Experimental Eye Research, 80*, 623–627.

Bhattacharyya, N., Darren, B., Schott, R. K., Tropepe, V., & Chang, B. S. W. (2017). Cone-like rhodopsin expressed in the all-cone retina of the colubrid pine snake as a potential adaptation to diurnality. *The Journal of Experimental Biology, 220*, 2418–2425. https://doi.org/10.1242/jeb.156430.
Boycott, B., & Wassle, H. (1999). Parallel processing in the mammalian retina: The Proctor Lecture. *Investigative Ophthalmology & Visual Science, 40*(7), 1313–1327.
Braekevelt, C. R. (1989). Photoreceptor fine structure in the bobtail goanna (*Tiliqua rugosa*). *Histology and Histopathology, 4*, 281–286.
Chen, M., & Goldsmith, T. H. (1986). Four spectral classes of cone in the retinas of birds. *Journal of Comparative Physiology, 159*, 473–479.
Collin, S. P., & Collin, H. B. (1999). The foveal photoreceptor mosaic in the pipefish, *Corythoichthyes paxtoni* (Syngnathidae, Teleostei). *Histology and Histopathology, 14*, 369–382.
Detwiler, S. R., & Laurens, H. (1920). Studies on the retina. The structure of the retina of *Phrynosoma cornutum*. *Journal of Comparative Neurology, 32*, 347–356.
Dieterich, C. E., Dieterich, H. J., & Hildebrand, R. (1976). Comparative electron-microscopic studies on the conus papillaris and its relationship to the retina in night and day active geckos. *Albrecht von Graefes Archiv fur Klinische und Experimentelle Ophthalmologie, 200*, 279–292.
Fernald, R. (2004). Evolving eyes. *The International Journal of Developmental Biology, 48*, 701–705.
Easter, S. S. (1992). Retinal growth in foveated teleosts: Nasotemporal asymmetry keeps the fovea in temporal retina. *Journal of Neuroscience, 12*, 2381–2392.
Fite, K. V., & Lister, B. C. (1981). Bifoveal vision in *Anolis* lizards. *Brain, Behavior and Evolution, 19*, 144–154.
Foureaux, G., Egami, M. I., Jared, C., Antoniazzi, M. M., Gutierre, R. C., & Smith, R. L. (2010). Rudimentary eyes of squamate fossorial reptiles (Amphisbaenia and Serpentes). *The Anatomical Record, 293*, 351–357.
Gerhing, W. J. (2014). The evolution of vision. *WIREs Developmental Biology, 3*, 1–40. https://doi.org/10.1002/wdev.96.
Hall, M. I. (2008). Comparative analysis of the size and shape of the lizard eye. *Zoology, 111*, 62–75.
Hall, M. I., & Ross, C. F. (2007). Eye shape and activity pattern in birds. *Journal of Zoology, 271*, 437–444.
Hetherington, T. E. (1989). Use of vibratory cues for detection of insect prey by the sandswimming lizard *Scincus scincus*. *Animal Behaviour, 37*, 290–297.
Hunt, D. M., & Collin, S. P. (2014). The Evolution of Photoreceptors and visual photopigments in vertebrates. In D. M. Hunt, M. W. Hankins, S. P. Collin, & N. J. Marshall (Eds.). *Evolution of Visual and Non-visual Pigments* (pp. 163–217). Springer-Verlag London Ltd.
Jones, M. P., Pierce, K. E., Jr., & Ward, D. (2007). Avian vision: A review of form and function with special consideration to birds of prey. *Journal of Exotic Pet Medicine, 16*(2), 69–87.
Kandilli, C., & Ulgen, K. (2008). Solar illumination and estimating daylight availability of global solar irradiance. *Energy Sources, 30*(12), 1127–1140.
Kelber, A., Vorobyev, M., & Osorio, D. (2003). Animal colour vision – behavioural tests and physiological concepts. *Biological Reviews, 78*, 81–118.
Kelber, A., & Lind, O. (2010). Limits of colour vision in dim light. *Ophthalmic and Physiological Optics, 30*(5), 454–459.
Kelber, A., Yovanovich, C., & Olsson, P. (2017). Thresholds and noise limitations of colour vision in dim light. *Philosophical transactions of the Royal Society of London B, 372*(1717), 20160065.
Kelber, A. (2019). Bird colour vision – from cones to perception. *Current Opinion in Behavioral Sciences, 30*, 34–40.
Khattab, F., Khattab, F. I., Fares, N., & Zaki, A. (2004). Retinal Photoreceptor Fine Structure in some reptiles. *The Egyptian Journal of Hospital Medicine, 17*, 167–186.
Kolb, H., & Dekorver, L. (1991). Midget ganglion cells of the parafovea of the human retina: A study by electron microscopy and serial section reconstructions. *Journal of Comparative Neurology, 303*, 617–636.
Kolb, H., & Marshak, D. (2003). The midget pathways of the primate retina. *Documenta Ophthalmologica, 106*(1), 67–81.
Koudouna, E., Winkler, M., Mikula, E., Juhasz, T., Brown, D. J., & Jester, J. V. (2018). Evolution of the vertebrate corneal stroma. *Progress in Retinal and Eye Research, 64*, 65–76.
Land, M. F. (2012). The Evolution of lenses. *Ophthalmic & Physiological Optics, 32*, 449–546.
Land, M. F., & Nilsson, D.-E. (Eds.). (2012). *Animal eyes*. Oxford University Press.
Makaretz, M., & Levine, R. L. (1980). A light microscopic study of the bifoveate retina in the lizard *Anolis carolinensis*: General observations and convergence ratios. *Vision Research, 20*, 679–686.
Malkemper, E. P., & Peichl, L. (2018). Retinal photoreceptor and ganglion cell types and topographies in the red fox (*Vulpes vulpes*) and Arctic fox (*Vulpes lagopus*). *Journal of Comparative Neurology, 526*, 2078–2098.
Malmström, T., & Kröger, R. H. H. (2006). Pupil shapesand lens optics in the eyes of terrestrial vertebrates. *The Journal of Experimental Biology, 209*, 18–25.
Mohun, S. M., Davies, W. L., Bowmaker, J. K., Pisani, D., Himstedt, W., Gower, D. J., ... Wilkinson, M. (2010). Identification and characterization of visual pigments in caecilians, a group of limb-less amphibians with rudimentary eyes from the Order Gymnophiona. *Journal of Experimental Biology, 213*, 3586–3592.
Moore, B. A., Tyrrell, L. P., Kamilar, J. M., Collin, S. P., Dominy, N. J., Hall, M. I., Heesy, C. P., Lisney, T. J., Loew, E. R., Moritz, G. L., Nava, S. S., Warrant, E., Yopak, K. E., & Fernández-Juricic, E. (2017). Structure and function of regional specializations in the vertebrate retina. Chapter 1.19. *Evolution of nervous systems* (pp. 351–372). Academic press.
Muntz, W. R. A. (1972). Inert absorbing and reflecting pigments. In H. J. A. Dartnall (Ed.). *Photochemistry of vision* (pp. 529–565). Berlin: Springer-Verlag.
Neumeyer, C. (1992). Tetrachromatic color vision in goldfish: Evidence from color mixture experiments. *Journal of Comparative Physiology, 171*, 639–649.
New, S. T. D., Hemmi, J. M., Kerr, G. D., & Bull, C. M. (2012). Ocular anatomy and retinal photoreceptors in a skink, the sleepy lizard (*Tiliqua rugosa*). *The Anatomical Record, 295*, 1727–1735.
Peichl, L., Behrmann, G., & Kroger, R. H. H. (2001). For whales and seals the ocean is not blue: A visual pigment loss in marine mammals. *European Journal of Neuroscience, 13*, 1520–1528.
Pietruszka, R. D., Hanrahan, S. A., Mitchell, D., & Seely, M. K. (1986). Lizard herbivory in a sand dune environment: The diet of *Angolosaurus skoogi*. *Oecologia, 70*, 587–591.
Polyak, S. (1941). *The retina.* Chicago: University of Chigaco Press.
Pyron, R. A., Burbrink, F. T., & Wiens, J. J. (2013). A phylogeny and revised classification of Squamata, including 4161 species of lizards and snakes. *BMC Evolutionary Biology, 13*, 93.
Querubin, A., Lee, H. R., Provis, J. M., & Bumsted O'Brien, K. M. (2009). Photoreceptor and ganglion cell topographies correlate with information convergence and high acuity regions in the adult pigeon (Columba livia) retina. *The Journal of Comparative Neurology, 517*, 711–722.
Robinson, M. D., & Cunningham, A. B. (1978). Comparative diet of two Namib desert sand lizards (Lacertidae). *Madoqua, 11*, 41–53.
Rodieck, R. W. (1998). *The First Steps in Seeing.* Sinauer Associates Inc Edition.
Röll, B. (2000). Gecko vision—visual cells, evolution, and ecological constraints. *Journal of Neurocytology, 29*, 471–484.
Röll, B. (2001a). Gecko vision—retinal organization, foveae and implications for binocular vision. *Vision Research, 41*, 2043–2056.
Röll, B. (2001b). Retina of Bouton's Skink (Reptilia, Scincidae): Visual Cells, Fovea, and Ecological Constraints. *The Journal of Comparative Neurology, 436*, 487–496.
Ruggeri, M., Major, J. C., Jr., McKeown, C., Knighton, R. W., Puliafito, C. A., & Jiao, S. (2010). Retinal structure of birds of prey revealed by ultra-high resolution spectral-domain optical coherence tomography. *Investigative Ophthalmology & Visual Science, 51*(11), 5789–5795.
Saleh, M. A. (1997). Amphibians and reptiles of Egypt. *Publication of the National Biodiversity Unit, 6*, 1–234.
Schachar, R. A., Pierscionek, B. K., & Le, T. (2007). The relationship between accommodative amplitude and the ratio of central lens thickness to its equatorial diameter in vertebrates eyes. *British Journal of Ophthalmology, 91*, 812–817.
Schott, R. K., Müller, J., Yang, C. G. Y., Bhattacharyya, N., Chan, N., Xu, M., ... Chang, B. S. W. (2016). Evolutionary transformation of rod photoreceptors in the all-cone retina of a diurnal garter snake. *Proceedings of the National Academy of Sciences, 113*(2), 356–361.
Seely, M. K. (1991). Sand dune communities. In G. A. Polis (Ed.). *The ecology of desert communities* (pp. 348–382). Tuscan: University of Arizona Press.
Stadler, A. T., Vihar, B., Günther, M., Huemer, M., Riedl, M., Shamiyeh, S., ... Baumgartner, W. (2016). Adaptation to life in aeolian sand: How the sandfish lizard, *Scincus scincus*, prevents sand particles from entering its lungs. *Journal of Experimental Biology, 219*, 3597–3604.
Stavenga, D. G., & Wilts, B. D. (2014). Oil droplets of bird eyes: Microlenses acting as spectral filters. *Philosophical Transactions of the Royal Society of London B, 369*, 20130041. https://doi.org/10.1098/rstb.2013.0041.
Taniguchi, Y., Hisatomi, O., Yoshida, M., & Tokunaga, F. (1999). Evolution of visual pigments in geckos. *Federation of European Biochemical Societies Letters, 445*, 36–40.
Vihar, B., Hanisch, F. G., & Baumgartner, W. (2016). Neutral glycans from sandfish skin can reduce friction of polymers. *Journal of the Royal Society Interface, 13*, 20160103. https://doi.org/10.1098/rsif.2016.0103.
Vorobyev, M. (2003). Coloured oil droplets enhance colour discrimination. *Proceedings of the Royal Society B London, 270*, 1255–1261.
Walls, G. (1942). *The vertebrate eye and its adaptive radiation.* Bloomfield Hills: Cranbrook Institute of Science.
Wilby, D., & Roberts, N. (2017). Optical influence of oil droplets on cone photoreceptor sensitivity. *The Journal of Experimental Biology, 220*, 1997–2004.
Yovanovich, C. A. M., Koskela, S. M., Nevala, N., Kondrashev, S. L., Kelber, A., & Donner, K. (2017). The dual rod system of amphibians supports colour discrimination at the absolute visual threshold. *Philosophical Transactions of the Royal Society of London B, 372*, 20160066.
Yovanovich, C. A. M., Pierotti, M. E. R., Rodrigues, M. T., & Grant, T. (2019). A dune with a view: The eyes of a neotropical fossorial lizard. *Frontiers in Zoology, 16*, 17. https://doi.org/10.1186/s12983-019-0320-2.
Zeigler, H. P., & Bischof, H. J. (1993). *Vision, brain and behavior in birds. A Bradford book.* Massachusetts Institute of Technology (MIT) Press.
Zhao, Z., Goedhals, J., Verdú-Ricoy, J., Jordaan, A., & Heideman, N. (2019). Comparative analysis of the eye anatomy in fossorial and surface- living skink species (Reptilia: Scincidae), with special reference to the structure of the retina. *Acta Zoologica, 00*, 1–13. https://doi.org/10.1111/azo.12297.